

MEMS-Reconfigurable Antenna based on a Multi-Size Pixelled Geometry

D. Rodrigo¹, Y. Damgaci², N. Biyikli², B.A. Cetiner², J. Romeu¹, L. Jofre¹

¹Signal Theory and Communications Department, Universitat Politècnica de Catalunya
Barcelona 08034 Spain
rodrigo@tsc.upc.edu

²Electrical and Computer Engineering, Utah State University
Logan UT 84322 Utah

Abstract— A MEMS reconfigurable antenna with beam steering capability and resonance frequency reconfigurability is presented. The design is based in an interconnected patch grid structure and employs a hybrid geometry with different sized patches in a biclustered distribution on order to reduce the structure complexity and the number of necessary switches. A small antenna of $\lambda/2$ by $\lambda/2$ using only 12 RF-MEMS switches is optimized using genetic algorithms, demonstrating beam tilting over a range of 120° and resonant frequency reconfigurability over 4, 5 and 6GHz. The described design constitutes a step forward in the accomplishment of multiple parameter reconfiguration.

I. INTRODUCTION

Present antennas, as part of a multimode multi-band communication system, are required to maintain performances under changing environment conditions or over different ranges of parameters. Instead of using a multiple of single-function legacy antennas, where each antenna is optimized for one of the different requirements, a single multifunctional reconfigurable antenna (MRA) can be employed. The behaviour of a reconfigurable antenna can be dynamically changed, thus a single antenna can accommodate multiple systems requirements. This is accomplished by modifying the current distribution, as a result of dynamic architectural changes.

Reconfigurable antenna parameters can be classified in two categories: impedance and radiation parameters. The first group refers to bandwidth and resonant frequency tuning, which are achieved by the electrical or physical modification of some critical dimension of the antenna, usually using capacitive loading or small structural modifications [1]-[2]. The second group controls polarization and radiation pattern and common techniques include parasitic elements modification and structural modifications preserving the main geometry [3]-[4].

To increase the reconfiguration capability achieving impedance and radiation reconfigurability simultaneously, poses a greater challenge which requires more general structures. Promising architectures are pixelled geometries, that consist of an electrically small patch grid interconnected by switches [5]-[6]. These structures, and thereby the antenna property, are modified by the activation/deactivation of the interconnecting switches. The main disadvantage of pixelled

geometries is the large number of necessary switches, reducing the antenna efficiency and requiring a higher reconfiguration time.

The purpose of this article is to present a novel reconfigurable antenna at 5.5 GHz based on a multisize pixelled geometry, focusing in the steering capability and resonant frequency modification while maintaining a low number of switches and a small size.

II. RECONFIGURABLE ANTENNA

A. Antenna Geometry

The antenna main geometry is depicted in Fig. 1 and consists on a grid of electrically small metallic patches. Some pairs of adjacent patches are interconnected by a switch. The activation or deactivation of these switches modifies the current distribution over the antenna surface providing reconfigurability to the antenna structure. The patch grid is located over a 30x40mm substrate vertically placed on a metallic ground plane and is fed through it using a coaxial probe. For this reason the antenna will be referred as *reconfigurable pixelled monopole*.

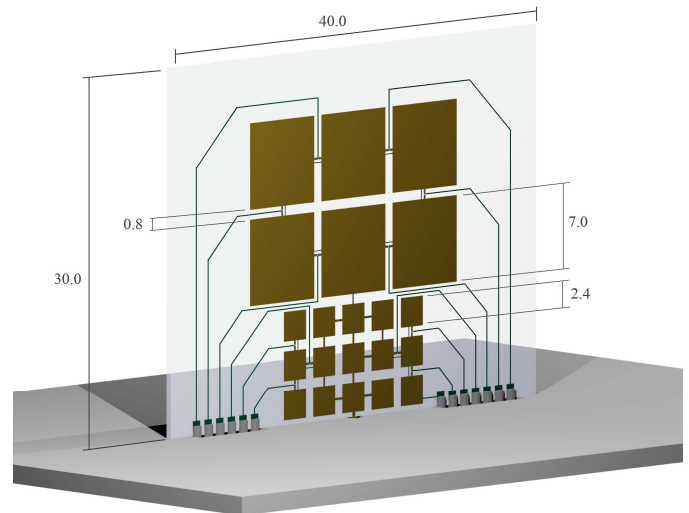


Fig. 1 Reconfigurable monopole antenna design (units in mm)

This type of antenna architecture is usually based on a uniform grid of constant size patches. However, the reconfiguration capabilities of the antenna can be enhanced by using a multi-size pixel distribution. The idea behind the present geometry is to locate the different reconfiguration capabilities on different antenna regions, dividing the antenna in different areas each one of them controlling one specific parameter of reconfiguration. When radiation pattern and input impedance are considered, it is convenient to allocate near to the feeding port the input impedance reconfiguration region since this parameter is mainly determined by the geometry surrounding the input port. On the other hand, the radiation pattern reconfiguration region is located near the input impedance region and it is kept as a parasitic area in order to minimize its influence over the antenna matching.

The advantage of this division of functionalities is that each region can be optimized independently according to its purpose. Since input impedance is very sensitive to any change of dimensions, the input impedance reconfiguration region is formed by small-size patches. On the other hand, to modify the antenna radiation pattern strong modifications over the current distribution are required, which makes more convenient the use of larger patches in its corresponding region.

The employment of a multi-size pixel geometry results in an optimized structure capable of modifying the frequency of operation and the radiation pattern, smaller in dimensions and with a lower number of switches than constant pixel size antennas.

B. Switching Mechanism

The switch is the element which provides reconfigurability to the antenna and its design and technology has a strong influence on the antenna performance. The recent developments of MEMS (nano/micro-electromechanical systems) technology allow a reliable and high yield implementation of RF-MEMS switches on high performance synthetic quartz substrate ($\epsilon_r=3.9$, $\tan\delta = 0.0002@10\text{GHz}$), providing a switching mechanism with low insertions losses and reasonable switching speed [7]. The interconnecting switches are single-arm RF-MEMS switches such as the one shown in Fig. 2. The typical dimensions are 150 microns length and 60 microns width. These switches activate with around 40V DC bias voltage applied through high resistance silicon chrome (SiCr) lines.

The use of synthetic quartz as substrate allows the integration of RF-MEMS switches without damaging the performance of the antenna, due to the quartz's moderate permittivity and low losses.

In order to determine the position of the switches, the contribution of each switch to the antenna reconfigurability has been analyzed by examining each switch status variability when a fully switched model is optimized to synthesize different radiation patterns and resonant frequencies. This criterion has been made compatible with the avoidance of vias in the biasing lines. These lines have been designed to cross the ground plane in order to place the biasing circuitry below

it, which also reduces their coupling with the antenna radiating structure.

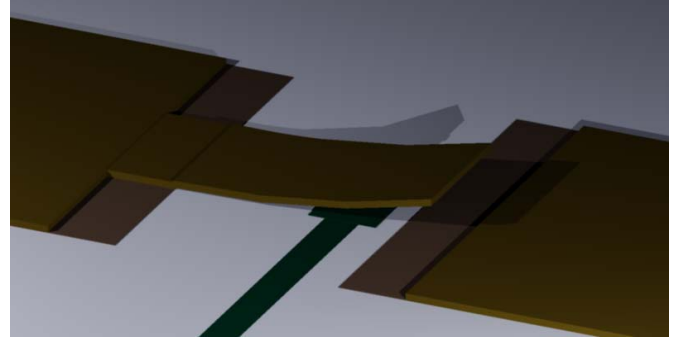


Fig. 2, Single-arm MEMS switch design

C. Optimization Process

The status of the RF-MEMS switches have been selected using a genetic algorithm in combination with rigorous EM full-wave analysis. The full-wave analyses of the reconfigurable pixelled monopole use the exact geometry of the single-arm cantilever type MEMS switches as well as high resistance silicon chrome (SiCr) DC bias lines, through which the actuation voltages are applied. Therefore, any possible EM coupling due to switch geometry and bias lines have been accounted for in the simulation results.

The fitness function employed by the genetic algorithm to evaluate the performance of a specific configuration depends on the parameter under reconfiguration. For resonant frequency reconfiguration, the fitness function corresponds to the return loss at the operation frequency. On the other hand, the fitness function for radiation pattern reconfigurability corresponds to the antenna gain in the steered direction including the losses due to non-perfect matching.

III. FREQUENCY RECONFIGURATION

The reconfigurable pixelled monopole has been originally designed to operate at 5.5 GHz. In this section, the antenna has been optimized for three different resonant frequencies: 4GHz, 5GHz and 6GHz. The simulated return loss curves are presented in Fig. 3 and the corresponding switch configurations are contained in Table I.

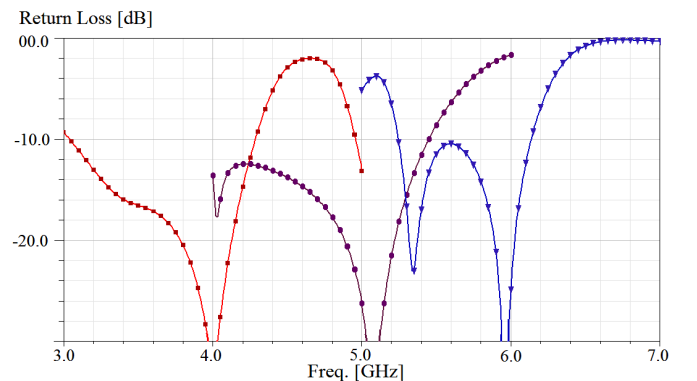


Fig. 3, Reflection coefficient of different resonant frequency configurations

The interpretation of the resulting configurations is often difficult, but in some cases is possible. For example, all the switches in the parasitic region of the 4GHz configuration are activated except one, creating an open loop of length 38mm, and since this length is approximately half the wavelength at 4GHz, the structure is resonant.

IV. RADIATION PATTERN RECONFIGURATION

Achieving radiation pattern reconfigurability for this antenna requires the joint operation of the two regions. The parasitic area modifies the direction of radiation, while the active area compensates the differences in the input impedance due to the coupling between the two areas.

The antenna has been reconfigured to radiate towards 4 different directions: -60° , -30° , 30° and 60° . The challenging step is to additionally maintain for each configuration a good matching over the considered band 5.47GHz to 5.825GHz (U-NII-2E and U-NII-3).

The simulated results in Fig. 4 prove the antenna to have the capability of steering the main beam for a range of 120° . In Fig. 5 it can be observed that the antenna is well matched over the whole bandwidth, having a value of -8dB in the worst case.

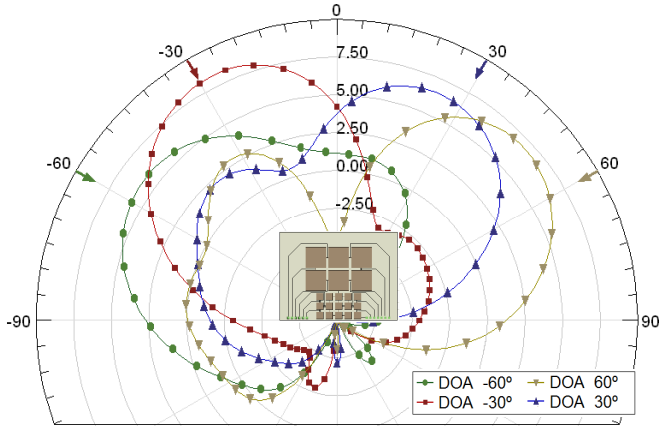


Fig. 4, Directivity of the different radiation pattern configurations

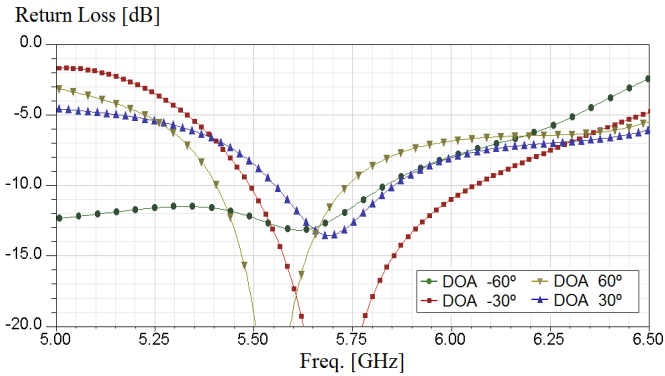


Fig. 5, Reflection coefficient of the different radiation pattern configurations

V. PROTOTYPE

To experimentally verify the results obtained in the previous section, a simpler switched prototype capable of steering the main beam to two different directions has been manufactured. Due to fabrication limitations, quartz glass has

been replaced for a common dielectric substrate with the most similar electromagnetic properties. The substrate used has been RO4003 ($\epsilon_r=3.55$, $\tan\delta=0.0027$) with a thickness of 0.813mm. The RF-MEMS used correspond to the model RMSW100 of RadantMEMS and the number of MEMS used has been reduced to 4. These switches have been connected using gold bondings and have been controlled using 100 V DC power supplies.

The high-resistance lines have been substituted by copper lines with serial inductances that reduce the coupling with the radiating elements of the antenna.

TABLE I
SWITCH CONFIGURATIONS

	Resonance Frequency			Radiation Pattern			
	4GHz	5GHz	6GHz	-60°	-30°	30°	60°
S ₁	0	1	0	0	1	0	0
S ₂	0	0	1	0	0	1	1
S ₃	0	1	0	1	0	0	0
S ₄	0	0	0	0	0	1	0
S ₅	1	0	1	0	1	0	1
S ₆	1	0	0	1	1	1	1
S ₇	1	1	1	0	1	0	0
S ₈	1	1	0	0	0	0	1
S ₉	1	1	0	1	1	1	1
S ₁₀	1	0	1	0	1	1	1
S ₁₁	1	0	1	0	0	1	1
S ₁₂	0	1	1	1	1	0	0

The prototype can be observed in Fig. 6, while RF-MEMS biasing details are represented in Fig. 7. The antenna is able to synthesize radiation patterns steered towards -30° and 30° . The first configuration results from activating switches 2 and 4, and the second configuration needs to active switches 1 and 3.

The measures relatives to the radiation pattern and reflection coefficient are presented in Fig.8 and Fig.9 respectively. It can be observed a good agreement between simulated and measured radiation patterns.

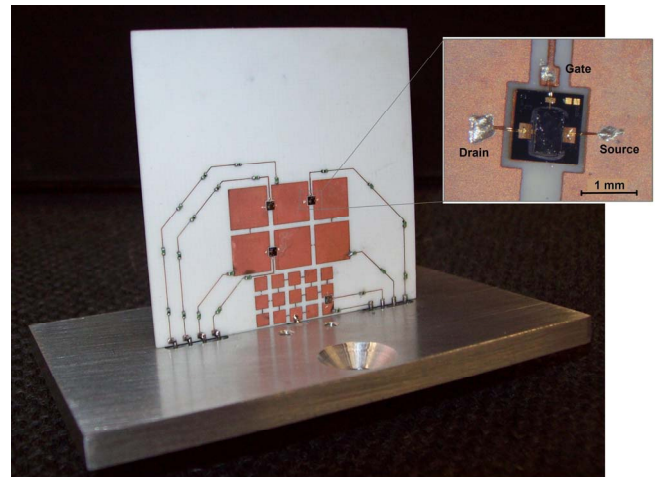


Fig. 6, Reconfigurable pixelled monopole prototype

VI. CONCLUSIONS

A MEMS reconfigurable antenna has been designed using a grid of interconnected small metallic patches, basing reconfigurability in the open or closed status of the switches placed between some specific pairs of adjacent patches. The employment of different sized patches has allowed simultaneous reconfiguration in frequency and radiation requiring only 12 RF-MEMS switches.

The MRA has been analyzed and optimized using the combination of genetic algorithms and fullwave simulations. By presenting different configurations, resonance frequency reconfiguration from 4GHz to 6GHz and beam-steering capability over 120 ° has been demonstrated.

A simpler prototype has been manufactured and measured, presenting a good agreement with simulated results.

ACKNOWLEDGMENT

This work was supported in part by the Spanish Interministerial Commission on Science and Technology (CICYT) under projects TEC2007-66698-C04-01/TCM and CONSOLIDER CSD2008-00068, by the Universitat Politècnica de Catalunya through the FPI-UPC Grant program.

REFERENCES

- [1] E. Erdil, K. Topalli, M. Unlu, O.A. Civi, and T. Akin. "Frequency Tunable Microstrip Patch Antenna Using RF MEMS Technology". *IEEE Transactions on Antennas and Propagation*, vol.55, No. 4, April 2007: 1193–1196.
- [2] R. Al-Dahleh, C. Shafai, and L. Shafai, "Frequency agile microstrip patch antenna using reconfigurable MEMS ground plane", *Microwave Optical Technol. Lett.*, Vol. 43, pp. 64–67, October 2004.
- [3] X. S. Yang, B. Z. Wang, W. Wu. "Pattern Reconfigurable Patch Antenna with Two Orthogonal Quasi-Yagi Arrays". *Antennas and Propagation Society International Symposium 2005, IEEE[C]*. 3-8 July 2005. Page(s): 617- 620 vol. 2B
- [4] C. W. Jung, M. J. Lee, G.P. Li, F. de Flaviis. "Reconfigurable Scan-Beam Single-Arm Spiral Antenna Integrated with RF-MEMS Switches". *IEEE Transactions on Antennas and Propagation*, vol. 54, no.2 February 2006: 455–463.
- [5] L. N. Pringle, P. H. Harms, S. P. Blalock, G. N. Kiesel, E. J. Kuster, P. G. Friederich, R. J. Prado, J. M. Morris, and G. S. Smith, "A reconfigurable aperture antenna based on switched links between electrically small metallic patches", *IEEE Trans. Antennas Propag.*, vol.52, pp.1434– 1445, June 2004.
- [6] J. C. Maloney, M. P. Kesler, L. M. Lust, L. N. Pringle, T.L. Fountain, P.H. Harms, G.S. Smith. "Switched fragmented aperture antennas". *Antennas and Propagation Society International Symposium, 2000. IEEE*. vol. 1, 16-21 July 2000 Page(s):310 – 313
- [7] Biyikli, N.; Damgaci, Y.; Cetiner, B.A., "Low-voltage small-size double-arm MEMS actuator," *Electronics Letters*, vol.45, no.7, pp.354-356, March 26 2009

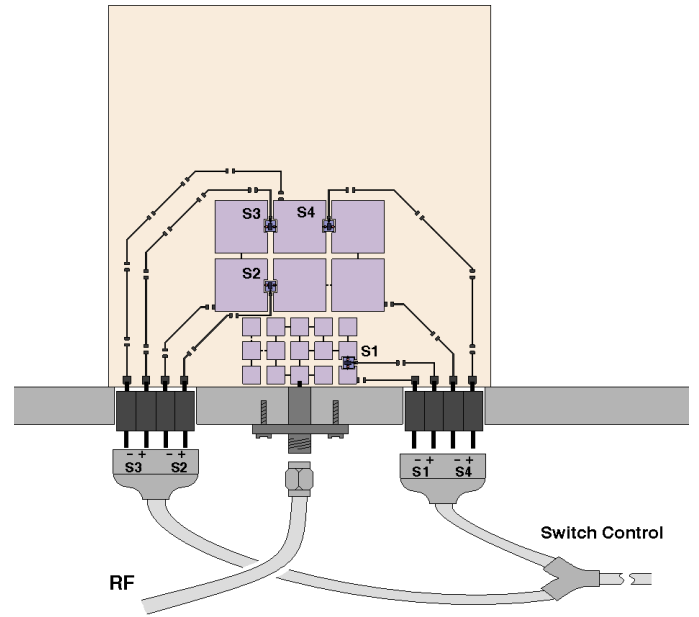


Fig. 7, Reconfigurable pixelated monopole, MEMS biasing details

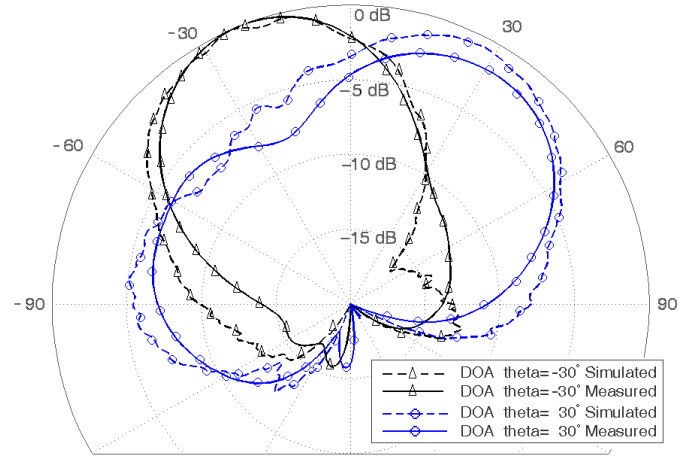


Fig. 8, Simulated and measured radiation pattern of the reconfigurable pixelated monopole prototype

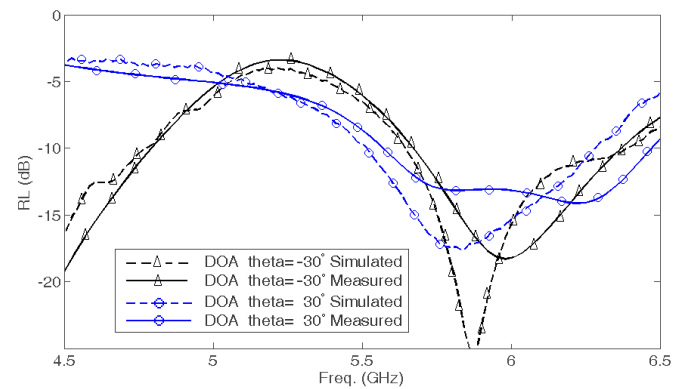


Fig. 9, Simulated and measured reflection coefficient of the reconfigurable pixelated monopole prototype